How to cite: *Angew. Chem. Int. Ed.* **2025**, e20563
doi.org/10.1002/anie.202520563

**Photoswitches**

# Azobenzene/Triptycene-Based Cholesteric Liquid Crystal Dopants

*Brandon Balamut*[+], *Kai Hanke*[+], *and Ivan Aprahamian**

**Abstract:** The noncovalent interactions in cholesteric liquid crystals (CLCs) can be modulated using switchable chiral dopants resulting in the phototuning of the reflected structural color. The nature of the interactions between the CLC and dopant, and how the latter can effectively transfer chiral information to the former is still somewhat of a black box. To gain insights into the nature of these interactions, we conducted structure–property analysis of five photoswitchable chiral dopants comprised of triptycene as the chiral core and azobenzene as the switchable unit. Our findings show that this combination results in high (e.g., 127 $\mu m^{-1}$) helical twisting power ($\beta$) values (i.e., extent of chiral information transfer between dopant and host), with dispersion interactions and/or electron deficient aromatic units playing a crucial role in determining the value. The large change in $\beta$ values upon *E/Z* photoswitching enabled us to devise multicolor, high contrast LC films that reflect across the UV to infrared light range.

Achieving precise and reversible control over self-assembled architectures is an essential prerequisite for creating new adaptive smart materials.[1–7] To this end the supramolecular interactions holding the assembly together need to be externally modulated. In the case of liquid crystals (LCs), for example, such manipulation can be achieved using switchable dopants,[8] resulting in the modulation of their (photo)physical properties.[9–11] The reason why this strategy works is because LCs are molecular amplifiers that propagate the slightest perturbation in their self-assembly from the meso to the macro scale.[12,13] This approach is at the core of the plethora of applications that LCs are used in, varying from display technologies,[14] sensors,[15] to tunable diffraction gratings,[16] and photopatterning,[17,18] among others.[19,20] In this respect, cholesteric liquid crystals (CLCs), formed by introducing chiral dopants into an achiral nematic LC host, thus imparting a helical twist in the otherwise linear aligned nematic mesogens, are of particular interest because of their unique optical properties, i.e., structural color. The periodic, helically-ordered structural phase of CLCs gives rise to selective reflection of light at specific wavelengths, determined by the refractive index ($n$) and the pitch ($P$) of the helical phase ($\lambda = nP$).[21] Aside from modifying the chiral dopant by using chemical[22–24] or electrical stimuli,[25,26] light, with its noninvasive and spatiotemporal resolution, has been used to this end, through the incorporation of chiral photoresponsive molecules into the LC.[27,28] While several molecular photoswitches,[29,30] (i.e., diarylethenes,[31] overcrowded alkenes,[32,33] and hydrazones[34–38]) have been used in controlling the properties of CLCs,[39,40] azobenzene[41–44] has the lion's share as it results in large helical twisting power values ($\beta$: ability to induce twisting in an achiral nematic LC), and large changes in $\beta$ ($\Delta\beta$)[11,13]). The latter is attributed to the large geometrical change azobenzene undergoes upon isomerization.

As for the chiral unit, in most cases, binaphthyl moieties have been used to achieve efficient chirality information transfer.[13,45] Recently,[37] to expand the structural landscape of chiral moieties that result in high $\beta$ values and to allow for structure property analyses that can yield insights as to why such units afford such values in the first place, we introduced triptycene[46–50] as a chiral motif for photoswitchable LC dopants. Our choice of this scaffold was based on its bent propeller-shape, extended $\pi$-surface, and high miscibility in nematic LC hosts,[51–53] which we thought would be a promising candidate for such use. To elaborate on the versatility of this moiety as a chiral scaffold, here, we report on the structure-property analysis of five new enantiomeric pairs of azobenzene-triptycene dopants (Figure 1) and detail the factors (e.g., electronic effects, van der Waals interactions, etc.) that influence their $\beta$ and $\Delta\beta$ values. The insights, gained from these studies and the comparison with the results obtained from hydrazone-based triptycene dopants, have helped us formulate new hypotheses on how to design efficient switchable chiral LC dopants (vide supra). Finally, we used the ability of the dopants to manipulate the reflected wavelengths in LC films from the UV to the near infrared (NIR) range (i.e., 420–1100 nm) to design new light and heat responsive multicolor LC canvases.

The chiral photochromic switches (**1–5**)[54] that we designed consist of a central triptycene scaffold connected via azo linkages to two substituted phenyl benzoate units (Figure 1a). The incorporation of the latter group was meant

[*] B. Balamut[+], Dr. I. Aprahamian
Department of Chemistry, Dartmouth College, 6128 Burke Laboratory, Hanover, NH 03755, USA
E-mail: ivan.aprahamian@dartmouth.edu
K. Hanke[+]
Institute of Organic Chemistry, Justus Liebig University Giessen, Heinrich-Buff-Ring 17, 35392 Giessen, Germany
K. Hanke[+]
Center for Materials Research (ZfM/LaMa), Justus Liebig University Giessen, Heinrich-Buff-Ring 16, 35392 Giessen, Germany
[+] Both authors contributed equally to this work.

Additional supporting information can be found online in the Supporting Information section


© 2025 Wiley-VCH GmbH

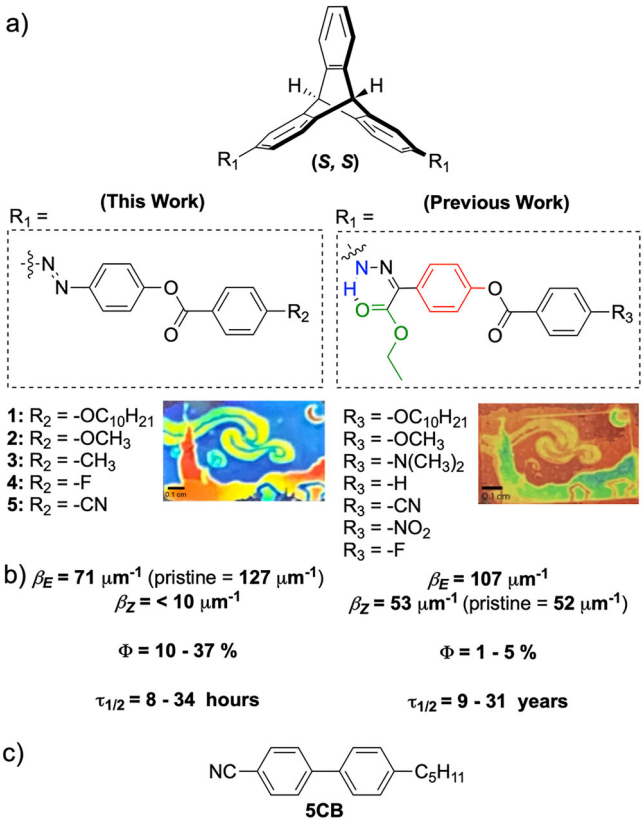


***Figure 1.*** a) The structures of the previously studied triptycene-based hydrazones (right), the newly developed azobenzene-based chiral dopants (left), and their use in drawing multi-color figures in LC films (for details see Supporting Information); "*The Starry Night*" by Vincent van Gogh (1889); copyright permission from The Museum of Modern Art/Licensed by SCALA/Art Resource, NY).[37] b) A comparison of the helical twisting power ($\beta$), the quantum yield ($\Phi$), and the thermal half-life ($\tau_{1/2}$) of the different families of dopants. c) The structure of the LC mesogen 5CB.

to extend the length of the chiral dopant to amplify the geometrical change upon photoisomerization and allow for a direct comparison with the previously studied triptycene-hydrazone counterparts.[37] To tease out electronic and dispersion effects on the $\beta$ and $\Delta\beta$ values, we also substituted this unit with $OC_{10}H_{21}$, $OCH_3$, $CH_3$, F, and CN groups. The synthesis, enantiomeric separation, and characterization of these dopants are described in the Supporting Information (Scheme S1 and Figures S1–35). The absolute configuration of the enantiomers was assigned by comparing their circular dichroism (CD) spectra with that of chiral dopant (***R,R***)**–1,** which we synthesized using enantiopure 2,6-*R,R*-diaminotriptycene (Figures S36–S42). The photophysical and photoisomerization properties of **1**–**5** were studied using UV–vis and $^1$H NMR spectroscopies (Figures S21–S35 and S43–S62, and Tables S1 and S2).

The absorption spectrum of the *EE* isomer of **1** displays the characteristic dual absorption band of azobenzene, with the more prominent one ($\lambda_{max}$ = 354 nm, $\varepsilon$ = 53700 $M^{-1}$ $cm^{-1}$) stemming from the $\pi-\pi*$ transition and the weaker one ($\lambda_{max}$ = 439 nm, $\varepsilon$ = 2550 $M^{-1}$ $cm^{-1}$) from the n$-\pi*$ transition. Irradiation of a pristine sample of **1** in toluene with 375 nm light affords a photostationary state (PSS) of 96% *Z*, which is accompanied with a decrease in the $\pi-\pi*$ band intensity and a slight increase and shift of the n$-\pi*$ one ($\lambda_{max}$ = 446 nm, $\varepsilon$ = 4310 $M^{-1}$ $cm^{-1}$). The isomerization process can be reversed by irradiation with 546 nm light, yielding a $PSS_{546}$ comprising of 91% of the *E* state. The quantum yields ($\Phi$) for the $EE \rightarrow ZZ$ isomerization of **1** (Figures S43–S46) and the reverse process were measured to be 11.6 ± 1.3% and 24.3 ± 0.9%, respectively, while the thermal isomerization half-life ($\tau_{1/2}$) was calculated to be 34.5 ± 0.8 h (Table S3). Compounds **2**–**5** (in both enantiomeric forms), exhibit similar photophysical properties, indicating that the functional groups at the terminal ends that are not in conjugation with the azo core, do not result in appreciable electronic effects (Table S2). The fatigue resistance of **1–5** was also studied, and minimal changes in absorption intensity were observed after 10 consecutive switching cycles (Figures S21–S35).

***Table 1:*** $\beta$ values ($\mu m^{-1}$) of the (*S,S*)[54] triptycene-based azobenzene dopants before and after light irradiation of the LC host 5CB.

| | $\beta_{pristine}$ | $\beta_{ZZ}$[a)] | $\beta_{EE}$[b)] |
|---|---|---|---|
| **1** | 127 | < 10 | 71 |
| **2** | 82 | < 10 | 66 |
| **3** | 89 | < 10 | 75 |
| **4** | 94 | < 10 | 80 |
| **5** | 107 | < 10 | 91 |

[a)] The $\beta$ values of the ZZ isomers at $PSS_{375}$ could not be measured as the helical pitch was too long to form disinclination lines using the Cano–method and so were estimated to be less than 10 $\mu m^{-1}$. [b)] The $\beta$ values were measured at $PSS_{546}$.

To study the effect of the triptycene-based dopants on the LC properties of achiral nematic hosts, **1–5** were doped into the LC host 5CB (Figure 1b,c) yielding cholesteric phases. The dopants showed excellent solubility in the nematic host and induced opposite handedness when doped with the enantiomeric pair (*R, R*) or (*S, S*). The $\beta$ values were measured using the Grandjean–Cano wedge method[55,56] (Figures S63–72 and Table S5) before and after irradiation with 375 and 546 nm light (Table 1). For example, the *EE* isomer of ***(S, S)*–1** in 5CB shows significant dopant-host interactions as evidenced by the large pristine $\beta$ value of 127 $\mu m^{-1}$ (Figure S63). Irradiation, with 375 nm light to obtain the *ZZ* rich state, increases the helical pitch and disrupts the CLC ensemble, making it difficult to accurately assess the $\beta$ and $\Delta\beta$ values. Assuming an upper limit of 10 $\mu m^{-1}$ for the $\beta$ value, the $\Delta\beta$ value will be 61 $\mu m^{-1}$ for **1**, which is substantial and key to achieving the wide-range reflection color tuning from the LC surface (vide infra). Back-isomerization through irradiation of the n–$\pi*$ band with 546 nm light restores the CLC phase yielding a $\beta$ value of 71 $\mu m^{-1}$, which is determined by the $PSS_{546}$ isomer ratio of 91:9 (i.e., it is not the same value as when pristine (99:1); Table S1). Heating the CLC mixture at 200 °C for 60 s completely re-equilibrates the switch reverting the $\beta$ value to 127 $\mu m^{-1}$.

A general trend with these dopants is that the *EE* isomers have larger $\beta$ values than their *ZZ* counterparts (Table 1).


© 2025 Wiley-VCH GmbH

15213773, 0, Downloaded from https://onlinelibrary.wiley.com/doi/10.1002/anie.202520563 by Justus-Liebig-Universitat, Wiley Online Library on [17/11/2025]. See the Terms and Conditions (https://onlinelibrary.wiley.com/terms-and-conditions) on Wiley Online Library for rules of use; OA articles are governed by the applicable Creative Commons License

This outcome results from the bent shape of the latter, which decreases the intermolecular interactions with the host LC. Exchanging the long decyloxy chain in **1** with a methoxy (**2**) or methyl (**3**) groups decreases the $\beta$ value for the pristine *EE* isomer by 45 and 38 $\mu m^{-1}$, respectively. We hypothesize that the shortening of the aliphatic functional group decreases the dispersion interactions between the dopant and 5CB, i.e., it is not caused by solubility differences. A similar effect was also observed in the triptycene–hydrazone switches highlighting the importance of dispersion interactions in such dopants. On the other hand, upon back isomerization with 546 nm light, the difference between the PSS and pristine $\beta$ values is much larger in **1** than **2**–**5**. We attribute this effect to the long alkyl chain in **1**, which causes a larger disorder in the LC in the *cis* form, even when present in small amounts at $PSS_{546}$ (i.e., 9%). The $\beta$ values of **2**, **3**, and **4** are similar, indicating that electronic effects are not playing a significant role in determining the values. This outcome is different from what we obtained with the triptycene-based hydrazone systems,[37] where significant differences in the $\beta$ values were observed by incorporating electron-donating and withdrawing functional groups at the terminal ends of the chiral dopants. This variation stems from the fact that electron withdrawing groups resulted in the destabilization of the CLC in both the *Z* and *E* forms (i.e., lowered the $\beta$ value), something not observed here, nor in the previously studied isosorbide-based hydrazone dopants.[36] Finally, dopant **5**, which has a CN group, and hence, a structural similarity with 5CB, has the second largest $\beta$ value of 107 $\mu m^{-1}$, a trend observed in the hydrazone-based system as well.[37] Finally, the hydrazone-based dopant results in much larger $\beta$ values than the azobenzene dopants using solely photoisomerization (e.g., 107 versus 71 $\mu m^{-1}$, respectively), but the azobenzene dopants achieve much higher $\beta$ values through thermal equilibration. This comparison highlights how even the smallest structural changes in such dopants can result in different properties and behavior especially across varying families of dopants. The results also show that the high $\beta$ value induction capability of triptycene is a general trend that is independent of the nature of the photoswitch, something which is not necessarily given in this research area.

To take advantage of the large $\beta$ value of **1,** we made light and heat responsive reflective films by loading doped (3 mol%) 5CB into planar aligned glass cells (5 and 10 µm cell thickness). The transmittance data (Figure 2) show excellent control over the reflection color from the visible to the NIR region, measured as a function of irradiation time with 375 followed by 546 nm light, allowing us to access surfaces that reflect the primary RGB colors (Figures 2a and S73–S87). The reason we initially used 515 nm light in the reflectance measurements is because it resulted in much faster isomerization to the *EE* state, allowing for more uniform transmittance bands and consistent structural color across the adaptive film. Next, 546 nm light was used to obtain a higher PSS value (91:9 versus 79:21) (Figure S21), yielding a further hypsochromic shift (Figure 2c) and hence better modulation of the reflected color.

Interestingly, the $\tau_{1/2}$ of the dopant is four times higher in the LC film than in toluene (i.e., 137 versus 35 h, respectively,

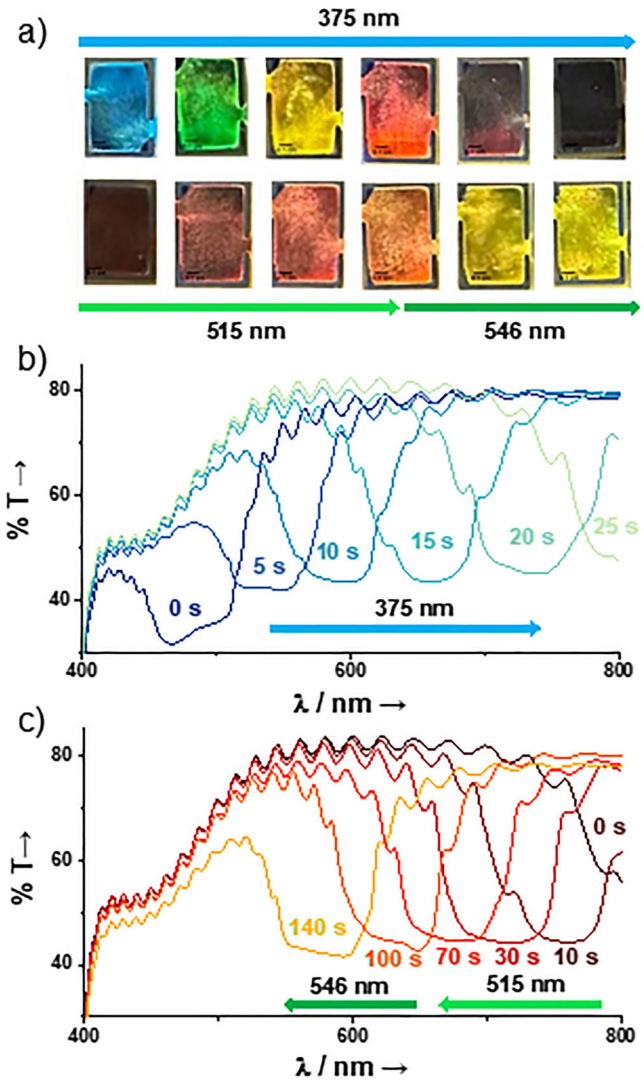


***Figure 2.*** a) Modulation of the structural color of 5CB doped with***(S, S)*–1** (3.0 mol%) in a LC 3–5 cell after irradiation with 375 followed by 515 and then 546 nm light. b) Irradiation-time dependent (375 nm) modulation of the bathochromic shift in reflectance wavelength of 5CB doped with **(*S*,*S*)-1** (3.0 mol%) starting with the pristine *EE* isomer and reaching $PSS_{375}$. c) Irradiation-time dependent (with 515 and then 546 nm) hypsochromic shift in reflectance modulation starting from $PSS_{375}$ to reach the end point.

see Tables S3 and S4), most likely because of the confinement of the photoswitch in the LC matrix. Literature reports are mixed[45,57] when it comes to the effect of the LC environment on the $\tau_{1/2}$ of azo switches and why sometimes the value increases while in others it decreases. To take advantage of the visible structural color reflection and relatively fast thermal isomerization of the switch, we used a combination of light irradiation and heat (200 °C) to draw, erase, and redraw various numbers in the same LC film using appropriate photomasks (Figure S88). This demonstration showcases an added benefit of these azo-based dopants as the short $\tau_{1/2}$ allows for fast reversion of the systems to their equilibrated state, something not easily achievable with the bistable hydrazones, resulting in a full reset of the system, and a


© 2025 Wiley-VCH GmbH

15213773, 0, Downloaded from https://onlinelibrary.wiley.com/doi/10.1002/anie.202520563 by Justus-Liebig-Universitat, Wiley Online Library on [17/11/2025]. See the Terms and Conditions (https://onlinelibrary.wiley.com/terms-and-conditions) on Wiley Online Library for rules of use; OA articles are governed by the applicable Creative Commons License


***Figure 3.*** Photomicrograph of our lab mascot Moby generated by the consecutive irradiation of 5CB doped with ***(S, S)*–1** (3.0 mol%) in a LC 3–5 cell with 394 nm light through two different grayscale masks for 10 s each.

higher isomer ratio than can be obtained at the PSS. The LC canvases can be reused even after months of preparation, show excellent fatigue resistance even after more than 20 write/erase cycles, and can be fully erased after heating to 200 °C for 60 s, showcasing their robustness. Finally, by sequentially applying more than one greyscale photomask and irradiating with 394 nm light in 5–10 s increments, we were able to phototune the *E*/*Z* isomer ratio at different parts of the film resulting in multi-colored images (Figures 3 and S88–S91) including our lab mascot, Moby, and Van Gogh's *Starry Night* (Scheme S1a and Figure S91). We decided to use 394 instead of 375 nm light in these experiments as the latter resulted in fast isomerization in the films and the entire visible spectrum was transversed in less than 7 s of irradiation (Figure S81). Irradiation with 394 nm light on the other hand resulted in slower isomerization, and hence, better control over the structural color modulation (Figure S82). This "painting" method is far more straightforward than the digital light processing technique we used earlier on to imprint multicolor images on LC canvases.[37] Considering the short $\tau_{1/2}$ of the azo switches, the imprinted figures last for 24 h before undergoing a hypsochromic shift that erases the detailed features of the painting, which is a disadvantage relative to the hydrazone-based systems, which showcase stable color reflection for days. Nonetheless, these dopants afford a fast write/erase cycle allowing its use in applications where information/color modulation is needed for short periods of time (e.g., rewriteable displays and smart surfaces as well as anti-counterfeiting, information storage, and security printing).[10,11]

In summary, we demonstrated the versatility of triptycene as a chiral scaffold by incorporating it in a series of azobenzene-based dopants. All the azo switches exhibit good bidirectionality, large Φ values, and tunable $\tau_{1/2}$ values from hours to days. When incorporated into the LC host 5CB, the large $\beta$ and $\Delta\beta$ values as well as the robustness of **1–5** allowed for repeated write/erase cycles of multicolored LC canvases. While there are other chiral dopants that give $\beta$ values exceeding 300 $\mu m^{-1}$, and $\Delta\beta$ values comparable to the ones reported herein,[41,58–62] the results obtained from the triptycene dopants are sufficiently large enough to enable the targeted applications with the added benefit of excellent photoswitching properties. Based on our structure/property analysis, in conjunction with data from the hydrazone-based dopants, the importance of dispersion interactions and structural similarity with the host LC in designing chiral dopants with large $\beta$ values is becoming evident. Overall, the works showcases the promise of triptycene as a new chiral scaffold in the photoswitchable LC and adaptive materials toolbox.

## Acknowledgements

This work was supported by the NSF program (DMR-2510040). B.B. acknowledges financial support from GAANN (P200A240037). K.H. acknowledges financial support from the Harris Program at Dartmouth for facilitating a research stay at the College. The authors are grateful to S. Bernhardt (Justus Liebig University) for help with the enantiomeric resolution of the chiral dopants using chiral HPLC.

## Conflict of Interests

The authors declare no conflict of interest.

## Data Availability Statement

The data that support the findings of this study are available in the Supporting Information of this communication.

**Keywords:** Azobenzene · Liquid crystals · Photoswitching · Structural color · Triptycene

[1] R. Zhang, A. Mozaffari, J. J. De Pablo, *Nat. Rev. Mater.* **2021**, *6*, 437–453. https://doi.org/10.1038/s41578-020-00272-x.
[2] F. A. Jerca, V. V. Jerca, R. Hoogenboom, *Nat. Rev. Chem.* **2021**, *6*, 51–69. https://doi.org/10.1038/s41570-021-00334-w.
[3] R. Costil, M. Holzheimer, S. Crespi, N. A. Simeth, B. L. Feringa, *Chem. Rev.* **2021**, *121*, 13213–13237. https://doi.org/10.1021/acs.chemrev.1c00340.
[4] C. Kaspar, B. J. Ravoo, W. G. Van Der Wiel, S. V. Wegner, W. H. P. Pernice, *Nature* **2021**, *594*, 345–355. https://doi.org/10.1038/s41586-021-03453-y.
[5] A. Leistner, Z. L. Pianowski, *Eur. J. Org. Chem.* **2022**, *2022*, e202101271.
[6] T. Aida, E. W. Meijer, *Isr. J. Chem.* **2020**, *60*, 33–47. https://doi.org/10.1002/ijch.201900165.
[7] L. Wang, A. M. Urbas, Q. Li, *Adv. Mater.* **2020**, *32*, 1801335. https://doi.org/10.1002/adma.201801335.
[8] A. Goulet-Hanssens, F. Eisenreich, S. Hecht, *Adv. Mater.* **2020**, *32*, 1905966. https://doi.org/10.1002/adma.201905966.
[9] J. Uchida, B. Soberats, M. Gupta, T. Kato, *Adv. Mater.* **2022**, *34*, 2109063. https://doi.org/10.1002/adma.202109063.
[10] M. E. McConney, M. Rumi, N. P. Godman, U. N. Tohgha, T. J. Bunning, *Adv. Opt. Mater.* **2019**, *7*, 1900429.
[11] H. K. Bisoyi, Q. Li, *Chem. Rev.* **2016**, *116*, 15089–15166. https://doi.org/10.1021/acs.chemrev.6b00415.
[12] L. J. Prins, P. Timmerman, D. N. Reinhoudt, *J. Am. Chem. Soc.* **2001**, *123*, 10153–10163. https://doi.org/10.1021/ja010610e.
[13] H. K. Bisoyi, Q. Li, *Chem. Rev.* **2022**, *122*, 4887–4926. https://doi.org/10.1021/acs.chemrev.1c00761.
[14] K. Yin, E.-L. Hsiang, J. Zou, Y. Li, Z. Yang, Q. Yang, P.-C. Lai, C.-L. Lin, S.-T. Wu, *Light Sci. Appl.* **2022**, *11*, 161. https://doi.org/10.1038/s41377-022-00851-3.


© 2025 Wiley-VCH GmbH

15213773, 0, Downloaded from https://onlinelibrary.wiley.com/doi/10.1002/anie.202520563 by Justus-Liebig-Universitat, Wiley Online Library on [17/11/2025]. See the Terms and Conditions (https://onlinelibrary.wiley.com/terms-and-conditions) on Wiley Online Library for rules of use; OA articles are governed by the applicable Creative Commons License

[15] A. Concellón, *Angew. Chem. Int. Ed.* **2023**, *62*, e202308857.
[16] A. Ryabchun, A. Bobrovsky, *Adv. Opt. Mater.* **2018**, *6*, 1800335. https://doi.org/10.1002/adom.201800335.
[17] R. S. Zola, H. K. Bisoyi, H. Wang, A. M. Urbas, T. J. Bunning, Q. Li, *Adv. Mater.* **2019**, *31*, 1806172. https://doi.org/10.1002/adma.201806172.
[18] H. Sakaino, D. J. Broer, S. C. J. Meskers, E. W. Meijer, G. Vantomme, *Angew. Chem. Int. Ed.* **2022**, *61*, e202200839. https://doi.org/10.1002/anie.202200839.
[19] A. Ryabchun, R. Jamagne, J. Echavarren, M. Patanapongpibul, L. Zhang, N. Katsonis, D. A. Leigh, *Chem* **2024**, *10*, 2196–2206. https://doi.org/10.1016/j.chempr.2024.03.013.
[20] S. Chen, N. Katsonis, D. A. Leigh, M. Patanapongpibul, A. Ryabchun, L. Zhang, *Angew. Chem. Int. Ed.* **2024**, *63*, e202401291. https://doi.org/10.1002/anie.202401291.
[21] H. Zhou, H. Wang, W. He, Z. Yang, H. Cao, D. Wang, Y. Li, *Molecules* **2022**, *27*, 4427. https://doi.org/10.3390/molecules27144427.
[22] S. J. D. Lugger, S. J. A. Houben, Y. Foelen, M. G. Debije, A. P. H. J. Schenning, D. J. Mulder, *Chem. Rev.* **2022**, *122*, 4946–4975. https://doi.org/10.1021/acs.chemrev.1c00330.
[23] L. Li, P. Jiang, X. Zhang, Y. Li, *Angew. Chem. Int. Ed.* **2025**, *64*, e202417149. https://doi.org/10.1002/anie.202417149.
[24] X. Su, S. Voskian, R. P. Hughes, I. Aprahamian, *Angew. Chem. Int. Ed.* **2013**, *52*, 10734–10739. https://doi.org/10.1002/anie.201305514.
[25] B. P. Radka, B. E. King, M. E. McConney, T. J. White, *Adv. Opt. Mater.* **2020**, *8*, 2000914. https://doi.org/10.1002/adom.202000914.
[26] Y. Itoh, D. Morishita, *Polym. J.* **2023**, *55*, 1035–1048. https://doi.org/10.1038/s41428-023-00805-5.
[27] H. K. Bisoyi, T. J. Bunning, Q. Li, *Adv. Mater.* **2018**, *30*, 1706512. https://doi.org/10.1002/adma.201706512.
[28] L. Wang, Q. Li, *Chem. Soc. Rev.* **2018**, *47*, 1044–1097. https://doi.org/10.1039/C7CS00630F.
[29] J. D. Harris, M. J. Moran, I. Aprahamian, *Proc. Natl. Acad. Sci. U.S.A.* **2018**, *115*, 9414–9422. https://doi.org/10.1073/pnas.1714499115.
[30] *Molecular Photoswitches: Chemistry, Properties, and Applications* (Ed: Z. L. Pianowski), Wiley-VCH: Weinheim **2022**.
[31] J. Hou, J. Wang, A. Ryabchun, B. L. Feringa, *Adv. Funct. Mater.* **2024**, *34*, 2312831. https://doi.org/10.1002/adfm.202312831.
[32] Z. Zheng, H. Hu, Z. Zhang, B. Liu, M. Li, D.-H. Qu, H. Tian, W.-H. Zhu, B. L. Feringa, *Nat. Photon.* **2022**, *16*, 226–234. https://doi.org/10.1038/s41566-022-00957-5.
[33] M. Fellert, R. Hein, A. Ryabchun, Y. Gisbert, C. N. Stindt, B. L. Feringa, *Angew. Chem. Int. Ed.* **2025**, *64*, e202413047.
[34] M. J. Moran, M. Magrini, D. M. Walba, I. Aprahamian, *J. Am. Chem. Soc.* **2018**, *140*, 13623–13627. https://doi.org/10.1021/jacs.8b09622.
[35] B. Shao, I. Aprahamian, *Chem* **2020**, *6*, 2162–2173.
[36] B. Balamut, R. P. Hughes, I. Aprahamian, *J. Am. Chem. Soc.* **2024**, *146*, 24561–24569. https://doi.org/10.1021/jacs.4c07848.
[37] I. Bala, J. T. Plank, B. Balamut, D. Henry, A. R. Lippert, I. Aprahamian, *Nat. Chem.* **2024**, *16*, 2084–2090. https://doi.org/10.1038/s41557-024-01648-0.
[38] B. Balamut, I. Aprahamian, *J. Am. Chem. Soc.* **2025**, *147*, 19444–19449. https://doi.org/10.1021/jacs.5c03668.
[39] Y. Kim, N. Tamaoki, *ChemPhotoChem* **2019**, *3*, 284–303. https://doi.org/10.1002/cptc.201900034.
[40] H. Wang, H. K. Bisoyi, X. Zhang, F. Hassan, Q. Li, *Chem. - Eur. J.* **2022**, *28*, e202103906.
[41] Y. Wang, Q. Li, *Adv. Mater.* **2012**, *24*, 1926–1945. https://doi.org/10.1002/adma.201200241.
[42] L. W. Giles, C. F. J. Faul, R. F. Tabor, *Mater. Adv.* **2021**, *2*, 4152–4164. https://doi.org/10.1039/D1MA00340B.
[43] W. Kang, Y. Tang, X. Meng, S. Lin, X. Zhang, J. Guo, Q. Li, *Angew. Chem. Int. Ed.* **2023**, *62*, e202311486. https://doi.org/10.1002/anie.202311486.
[44] H. Wang, Y. Tang, H. K. Bisoyi, Q. Li, *Angew. Chem. Int. Ed.* **2023**, *62*, e202216600.
[45] X. Zhang, Y. Tang, Y. Ma, H. K. Bisoyi, T. Li, Q. Li, *Adv. Funct. Mater.* **2025**, *35*, 2425752. https://doi.org/10.1002/adfm.202425752.
[46] A. Kunz, N. Oberhof, F. Scherz, L. Martins, A. Dreuw, H. A. Wegner, *Chem. Euro. J.* **2022**, *28*, e202200972. https://doi.org/10.1002/chem.202200972.
[47] A. Lohr, T. M. Swager, *J. Mater. Chem.* **2010**, *20*, 8107–8111. https://doi.org/10.1039/c0jm00621a.
[48] M.d. N. Khan, T. Wirth, *Chem. Euro. J.* **2021**, *27*, 7059–7068. https://doi.org/10.1002/chem.202005317.
[49] F. Ishiwari, Y. Shoji, C. J. Martin, T. Fukushima, *Polym. J.* **2024**, *56*, 791–818. https://doi.org/10.1038/s41428-024-00920-x.
[50] M. Zharnikov, Y. Shoji, T. Fukushima, *Acc. Chem. Res.* **2025**, *58*, 312–324. https://doi.org/10.1021/acs.accounts.4c00743.
[51] S. Norvez, *J. Org. Chem.* **1993**, *58*, 2414–2418. https://doi.org/10.1021/jo00061a012.
[52] S. Norvez, J. Simon, *Liq. Cryst.* **1993**, *14*, 1389–1395. https://doi.org/10.1080/02678299308026451.
[53] T. M. Long, T. M. Swager, *J. Mater. Chem.* **2002**, *12*, 3407–3412. https://doi.org/10.1039/B203160D.
[54] We have synthesized and fully characterized both the RR and the SS enantiomers of the dopants. Considering that in all cases the photophysical and LC characterization results are very similar (Table S5), our discussion here will focus on the SS enantiomers. Our choice stems from the fact that the SS is slightly more enantiopure, yielding slightly higher $\beta$ values (Scheme S1).
[55] T.-T. Tang, H.-Y. Wu, C.-J. Lin, R.-P. Pan, *Mol. Cryst. Liq. Cryst.* **2007**, *478*, 899–906. https://doi.org/10.1080/15421400701681745.
[56] D. Podolskyy, O. Banji, P. Rudquist, *Liq. Cryst.* **2008**, *35*, 789–791. https://doi.org/10.1080/02678290802175756.
[57] A. Miniewicz, H. Orlikowska, A. Sobolewska, S. Bartkiewicz, *Phys. Chem. Chem. Phys.* **2018**, *20*, 2904–2913. https://doi.org/10.1039/C7CP06820D.
[58] Y. Li, C. Xue, M. Wang, A. Urbas, Q. Li, *Angew. Chem. Int. Ed.* **2013**, *52*, 13703–13707. https://doi.org/10.1002/anie.201306396.
[59] L. Qin, W. Gu, J. Wei, Y. Yu, *Adv. Mater.* **2018**, *30*, 1704941. https://doi.org/10.1002/adma.201704941.
[60] T. Ube, M. Yoshida, S. Kurihara, T. Ikeda, *ACS Appl. Mater. Interfaces* **2024**, *16*, 28638–28644. https://doi.org/10.1021/acsami.4c04370.
[61] X. Zhang, B. Koz, H. K. Bisoyi, H. Wang, K. G. Gutierrez-Cuevas, M. E. McConney, T. J. Bunning, Q. Li, *ACS Appl. Mater. Interfaces* **2020**, *12*, 55215–55222. https://doi.org/10.1021/acsami.0c19527.
[62] J. Sheng, D. R. S. Pooler, B. L. Feringa, *Chem. Soc. Rev.* **2023**, *52*, 5875–5891. https://doi.org/10.1039/D3CS00247K.

Manuscript received: September 18, 2025
Revised manuscript received: October 15, 2025
Manuscript accepted: October 17, 2025
Version of record online: ■■, ■■


© 2025 Wiley-VCH GmbH

15213773, 0, Downloaded from https://onlinelibrary.wiley.com/doi/10.1002/anie.202520563 by Justus-Liebig-Universitat, Wiley Online Library on [17/11/2025]. See the Terms and Conditions (https://onlinelibrary.wiley.com/terms-and-conditions) on Wiley Online Library for rules of use; OA articles are governed by the applicable Creative Commons License